Available online at www.sciencedirect.com

ScienceDirect

Biomedical Journal

journal homepage: www.elsevier.com/locate/bj

Original Article

AIFM1, negatively regulated by miR-145-5p, aggravates hypoxia-induced cardiomyocyte injury

Wugang Zhou [a,b,1], Lv Ji [b,1], Xuqin Liu [b], Dan Tu [b], Ningning Shi [b], Wangmu Yangqu [b], Shi Chen [c,d], Pingjin Gao [e,f,g], Hong Zhu [h,*], Chengchao Ruan [e,f,g,**]

[a] Department of Emergency, Shanghai Ninth People's Hospital, School of Medicine, Shanghai Jiao Tong University, Shanghai, China
[b] Department of Intensive Care Unit, Shigatse People's Hospital, Shigatse, Tibet Autonomous Region, China
[c] Key Laboratory of Combinatorial Biosynthesis and Drug Discovery Ministry of Education, School of Pharmaceutical Sciences, Wuhan University, Wuhan, Hubei, China
[d] Brain Center, Zhongnan Hospital, Wuhan University, Wuhan, Hubei, China
[e] State Key Laboratory of Medical Genomics, Shanghai Key Laboratory of Hypertension, Ruijin Hospital, Shanghai Jiao Tong University School of Medicine, Shanghai, China
[f] Department of Hypertension, Shanghai Institute of Hypertension, Ruijin Hospital, Shanghai Jiao Tong University School of Medicine, Shanghai, China
[g] Key Laboratory of Stem Cell Biology, Shanghai Institutes for Biological Sciences, Chinese Academy of Sciences, Shanghai, China
[h] Clinical Medical School, Shanghai Ninth People's Hospital, School of Medicine, Shanghai Jiao Tong University, Shanghai, China

ARTICLE INFO

Article history:
Received 28 October 2020
Accepted 25 November 2021
Available online 1 December 2021

Keywords:
AIFM1
miR-145-5p
Myocardial infarction
Hypoxia-induced cardiomyocyte injury

ABSTRACT

Background: Hypoxia-induced apoptosis is linked to the pathogenesis of myocardial infarction. The role of apoptosis-inducing factor mitochondria associated 1 (AIFM1) in cardiomyocyte injury remains unclear. This study was aimed at probing into the role and the underlying regulatory mechanism of AIFM1 in myocardial injury.

Methods: H9c2 cardiomyocytes and C57BL/6 mice were used for myocardial hypoxic/ischemic injury and myocardial infarction animal models. Quantitative real-time polymerase chain reaction (qRT-PCR) was performed to evaluate the expression levels of AIFM1 mRNA and miR-145-5p. Western blot was used for examining the expression levels of AIFM1, caspase-3, cleaved caspase-3, p-53, and γ-H2AX. Cell viability was examined by cell counting kit-8 (CCK-8) assay and BrdU assay. Interaction between AIFM1 and miR-145-5p was determined by bioinformatics analysis, qRT-PCR, Western blot, and dual-luciferase reporter assay.

* *Corresponding author*. Clinical Medical School, Shanghai Ninth People's Hospital, School of Medicine, Shanghai Jiao Tong University, Room 401, Building 1, Jinzun Rd. 115, Pudong Dist., Shanghai 200125, China.
** *Corresponding author*. Department of Hypertension, Shanghai Institute of Hypertension, Ruijin Hospital, Shanghai Jiao Tong University School of Medicine, Ruijin 2nd Rd. 197, Shanghai 200024, China.
E-mail addresses: zhuhong1096@163.com (H. Zhu), lin525925855815811@163.com (C. Ruan).
Peer review under responsibility of Chang Gung University.
[1] Contributed equally.
https://doi.org/10.1016/j.bj.2021.11.012

Results: AIFM1 expression was markedly highly elevated, while miR-145-5p expression was significantly down-regulated in the myocardial infarction animal model and H9c2 cells under hypoxia. Augmentation of AIFM1 led to a dramatic decrease of cell viability, accompanied by an increase of the secretion of the inflammatory cytokines IL-1β, TNF-α, IL-6, and the expression of cleaved caspase-3. Furthermore, AIFM1 was identified as a target of miR-145-5p. In addition, miR-145-5p/AIFM1 axis regulated the expression of p53. *Conclusion:* AIFM1 may exacerbate myocardial ischemic injury by promoting inflammation and the injury of cardiomyocytes, and its up-regulation may be partly due to the down-regulation of miR-145-5p.

At a glance commentary

Scientific background on the subject

AIFM1 has a role in the development of multiple diseases. However, the role of AIFM1 in myocardial infarction (MI) remains unclear.

What this study adds to the field

We found that AIFM1 expression was markedly highly elevated in the myocardial infarction animal model and H9c2 cells under hypoxia. AIFM1 overexpression inhibited cell viability, and promote the secretion of the inflammatory cytokines IL-1b, TNF-α, IL-6, and the expression of cleaved caspase-3. Furthermore, AIFM1 was identified as a target of miR-145-5p, and miR-145-5p/AIFM1 axis regulated the expression of p53.

Myocardial infarction (MI) is one of the important causes of cardiac death. Although great progress has been made in modern medicine over the past decades, acute myocardial infarction (AMI) is still one of the leading killers worldwide [1–3]. In addition, a lot of studies authenticate that ischemia/hypoxia is responsible for the damage to cardiomyocytes as well as complicated pathological and physiological changes in which many molecules play important roles. Nevertheless, the curative efficacy for cardiac failure, cardiac remodeling, and other problems resulted from MI is unsatisfactory [4,5]. Therefore, identifying highly sensitive and specific molecular markers has great significance for the search of new therapeutic targets for MI.

MicroRNAs (miRNAs), a class of non-coding RNAs with a length of about 20–25 nt, play a prominent role in cell proliferation, apoptosis, differentiation, regeneration, and other processes. An increasing number of miRNAs are found to exert vital functions on the pathological events following MI and regarded as potential therapeutic targets. For example, miR-188-3p expression is found to be abnormally down-regulated in cardiomyocytes after anoxia/reoxygenation, regulating the autophagy and apoptosis of cardiomyocytes [6]; miR-34a expression is increased following MI and miR-34a inhibits the recovery of the cardiac function [7]; miR-873 plays an important role in reducing the myocardial infarction area [8]. Moreover, miR-145-5p is found to be closely associated with cardiovascular diseases. For example, miR-145-5p is involved in the proliferation and migration of vascular smooth muscle cells [9,10]. In myocardial ischemia-reperfusion injury, miR-145-5p regulates hypoxia-induced inflammatory reactions by targeting CD40, thereby modulating the apoptosis of cardiomyocytes [11]. MiR-145-5p can promote the apoptosis of cardiomyocytes by repressing dual-specificity phosphatase 6 (DUSP6) [12]. However, the mechanism through which miR-145-5p plays a role in MI has not been fully clarified.

Apoptosis-inducing factor mitochondria associated 1 (AIFM1), a protein whose gene is located on chromosome Xq26.1, is closely associated with ventriculomegaly, muscular atrophy, and other human diseases [13,14]. When cells are subjected to apoptosis and injury, the 62 kDa AIFM1 is spliced into a 57 kDa truncated AIFM1 and released from mitochondria to cytoplasm and nuclei, which induces two typical caspase-independent apoptosis phenomena: chromosome condensation and fracture of large DNA fragments. AIFM1 mutation often results in myopathy or mitochondrial diseases [15]. However, the role of AIFM1 in hypoxia-induced myocardial injury is still obscure.

In the present work, we found that AIFM1 was one of the potential targets of miR-145-5p by searching TargetScan database (http://www.targetscan.org/vert_72/), and we investigated the functions of miR-145-5p and AIFM1 in hypoxia-induced myocardial injury to lay a theoretical foundation for the occurrence and development of MI and ischemia/hypoxia related diseases, and to explore novel therapeutic targets on this basis.

Materials and methods

Cell culture and transfection

H9c2 cardiomyocytes were purchased from the American Type Culture Collection (ATCC) (Manassas, VA, USA) and cultured in RPMI-1640 medium (Gibco, Grand Island, NY, USA) containing 10% fetal bovine serum (FBS, Gibco, Grand Island, NY, USA) and 100 U/ml penicillin, 100 μg/ml streptomycin (Gibco, Grand Island, NY, USA) in a thermostatic incubator at 37 °C in 5% CO_2. When the confluency of H9c2 cells reached 80%, these cells were further cultured in an incubator in 5% CO_2 for 12 h, and then the incubator was filled with 99.9% N_2

gas. O_2 volume fraction <1% determined by a monitor was considered as hypoxic status.

pcDNA3.1 plasmid was used to construct the AIFM1 overexpression vector, and shRNA against AIFM1 (AIFM1 shRNA) was used to construct AIFM1 knockdown model. As for transfection, negative control vector (NC), pcDNA3.1-AIFM1, AIFM1 shRNA, miR-145-5p mimics, miR-145-5p inhibitors, and their controls (mimics NC and inhibitors NC) were available from GenePharma (Shanghai, China). All the plasmids or oligonucleotides were transfected at a final concentration of 50 nM and H9c2 cells were inoculated into a 24-well cell culture plate at a density of 3×10^5 cells/well. According to the supplier's instruction, Lipofectamine® 3000 (Invitrogen, Carlsbad, CA) was used to transfect the plasmids or oligonucleotides mentioned above into H9c2 cells. 24 h after the transfection, the transfection efficiency was detected by quantitative real-time polymerase chain reaction (qRT-PCR).

Establishment of a mouse model of MI

Sixty 8-week-old male C57BL/6 mice (from the Department of Laboratory Animal Science, Peking University Health Science Center, Beijing, China) were selected to construct a mouse model of MI with the method as previously described [16]. In brief, the mice were anesthetized by isoflurane. Left thoracotomy was performed in the 4th intercostal space, and the pericardium was gently torn with microscope forceps to expose the left anterior descending coronary artery which was then sutured with 8-0 atraumatic suture. Myocardial whitening and reduced myocardial motion in and below the ligation position were the signs of successful modeling. All the operations above were executed on a thermostatic pad at 37 °C. For the sham-operation group, the surgical suture was used in the corresponding position, but the ligation was not performed. To explore the effects of miR-145-5p on cardiac functions and left ventricle remolding, miR-145-5p mimics, miR-145-5p inhibitors, or their negative controls were intravenously injected into the tail vein of mice two weeks (80 μg/g) before ligation, respectively. Three days after ligation, all the mice were killed with an anesthetic and myocardial tissues were harvested. The experimental protocol of this study was endorsed by the Ethics Committee of Shanghai Ninth People's Hospital.

qRT-PCR

Total RNA was extracted from plasma and cells with TRIzol (Invitrogen, Carlsbad, CA). After RNA concentration and purity were detected by Thermo Scientific™ NanoDrop™ One spectrophotometer, PrimeScript RT Reagent (TaKaRa, Tokyo, Japan) was adopted to reversely transcribe RNA into cDNA. With cDNA as the template, qRT-PCR was conducted using an ABI 7500 Real-time PCR System (Applied Biosystems, Carlsbad, CA, USA) with SYBR Green Master Mix (Roche, Shanghai, China). The reaction conditions were as below: denaturation at 95 °C for 15 s, annealing at 55 °C for 30 s, and extension at 72 °C for 10 s. A total of 35 cycles of amplification were performed. Relative expression levels of the genes were quantified by the $2^{-\triangle\triangle Ct}$ method. The primers used were shown in Table 1.

Table 1 The primers used for PCR in this study.

Name	Primer sequences
miR-145-5p	Forward: 5′-GTCCAGTTTTCCCAGGAATC-3′ Reverse: 5′-AGAACAGTATTTCCAGGAAT-3′
AIFM1	Forward: 5′-TCTGGACACTGGCAAACATC-3′ Reverse: 5′-GCTTTCCCCAGAAAGACACA-3′
U6	Forward: 5′-CTCGCTTCGGCAGCACATATACT-3′ Reverse: 5′-ACGCTTCACGAATTTGCGTGTC-3′
GAPDH	Forward: 5′-GCAAGTTCAACGGCACAG-3′ Reverse: 5′-GCCAGTAGACTCCACGACAT-3′

Western blot

RIPA solution (Beyotime Biotechnology, Shanghai, China) containing protease inhibitor was used to lyse the cells and extract total protein. Protein concentration was determined employing a BCA protein assay kit (Pierce, Appleton, WI, USA). Following that, the protein samples were mixed with loading buffer, denatured in boiling water, and separated by 10% sodium dodecyl sulfate-polyacrylamide gel electrophoresis (SDS-PAGE). After SDS-PAGE, the protein samples were transferred onto a nitrocellulose (NC) membrane. Following that, the membrane was blocked in 5% skim milk for 1 h at room temperature. Then the membrane was placed on the rocker at ambient temperature for incubation with primary antibody (anti-AIFM1, rabbit polyclonal antibody, 1: 1,000, Solarbio, K003425P; anti-caspase-3, rabbit monoclonal antibody, 1: 1,000, Abcam, ab32351; anti-cleaved caspase-3, rabbit monoclonal antibody, 1: 1,000, Abcam, ab32042; anti-p53, rabbit monoclonal antibody, 1: 1,000, Abcam, ab32389; anti-γ-H2AX, rabbit monoclonal antibody, 1: 1,000, Abcam, ab229914) for 1 h. After being rinsed with TBST solution, the membrane was incubated with secondary antibody (goat anti-rabbit polyclonal antibody, 1:6,000, Abcam, ab205781) at ambient temperature for 1 h before the rinse with TBST solution again. Ultimately, color rendering was performed using hypersensitive ECL (Biossci Biotechnology Co, Ltd., Wuhan, China).

Dual-luciferase reporter gene assay

The target sequence of AIFM1 3′UTR for miR-145-5p was predicted based on TargetScan. Wild type (WT) AIFM1 sequence and mutant type (MUT) AIFM1 sequence were sub-cloned into pGL3 expression vectors (Promega, Madison, WI, USA), respectively, and the luciferase reporter vectors were transfected to H9c2 cells and then inoculated in 24-well plates (1×10^5 cells/well). Then miR-145-5p mimics (or mimics NC) were co-transfected into H9c2 cells. Luciferase activity was determined by a dual-luciferase reporter system (Promega, Madison, WI, USA) after 48 h.

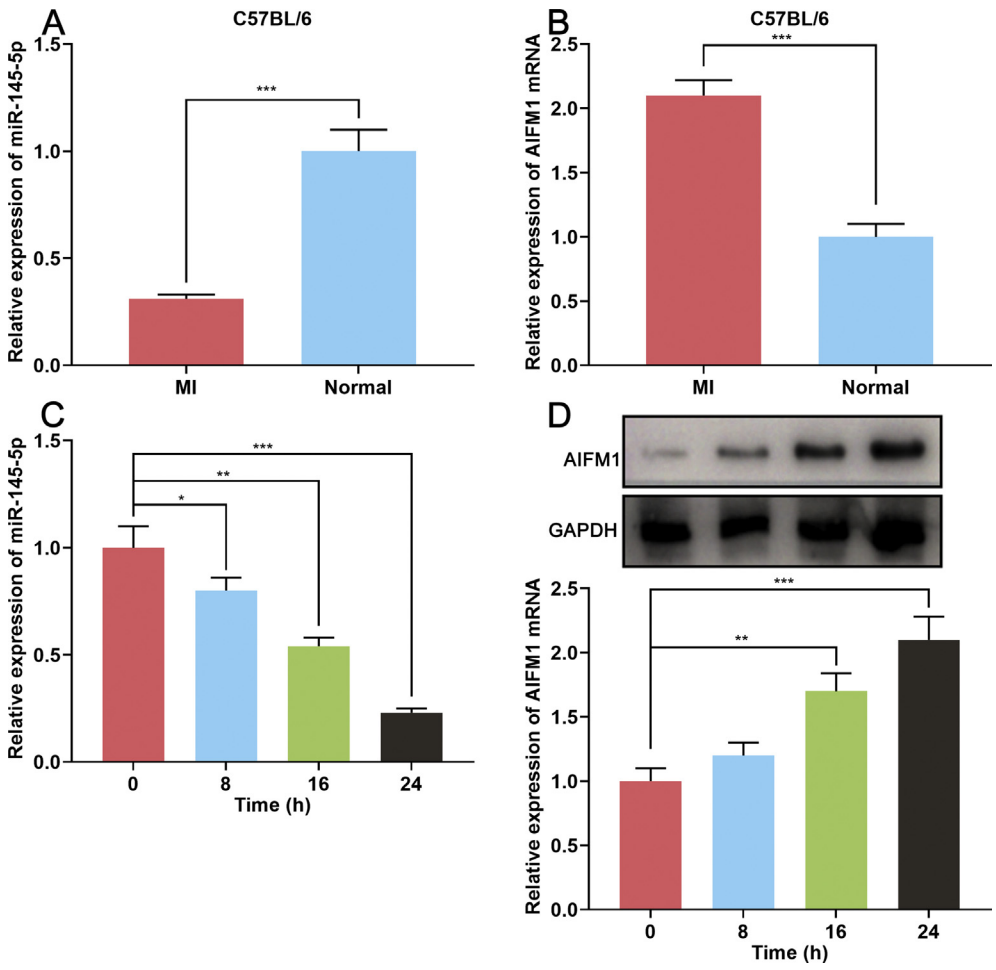

Fig. 1 **The expression levels of miR-145-5p and AIFM1 in mice with MI or H9c2 cells subjected to hypoxia**. (A–B) The expression levels of miR-145-5p and AIFM1 mRNA in the myocardial tissue of C57BL/6 mice with MI or sham-operation (n = 10 in each group) were detected by qRT-PCR. (C–D) The expression levels of miR-145-5p and AIFM1 in H9c2 cells subjected to hypoxia for 0, 8, 16, or 24 h were detected by qRT-PCR and Western blot. *$p < 0.05$, **$p < 0.01$, and ***$p < 0.001$.

BrdU assay

The medium of the cells in each group was discarded, and 1 × BrdU labeling medium was used to incubate the cells for 1 h in an incubator according to the instructions of BrdU cell proliferation assay kit (Roche, Shanghai, China). Anti-BrdU mouse monoclonal antibody was used to incubate the cells at room temperature for 1 h, and goat anti-mouse secondary antibody (Beyotime, Shanghai, China) was then added to incubate the cells at room temperature for another 1 h. Subsequently, DNA counterstaining was performed with DAPI staining solution. Ultimately, BrdU-positive cells (in green light) were observed and counted under an inverted fluorescence microscope.

Cell counting kit-8 (CCK-8) assay

When the rate of cell confluency reached about 80%, H9c2 cells were prepared to cell suspension before being inoculated in a 96-well plate (5×10^3 cells/well, 100 μL). One group was given normal culture, while other groups were placed in 1% O_2 hypoxic incubators for 4 h, 8 h, 16 h, and 24 h of culture, respectively. Then the 96-well plates were taken out. After that, each well was added with 10 μL of CCK-8 solution (Biossci Biotechnology Co, Ltd., Wuhan, China), and then the cells were incubated for another 1 h. Optical density (OD) at 450 nm was measured by a microplate reader (Bio-Rad Laboratories, Inc., Hercules, CA, USA). Cell viability = (OD of hypoxic cells - OD of blank control)/(OD of normal cells - OD of blank control) × 100%.

LDH cytotoxicity assay

The level of LDH secreted by cells was determined by the LDH cytotoxicity assay kit (Beyotime Biotechnology, Shanghai, China). Cell culture solution was collected, and then there was blank well (25 μL double distilled water), standard well (5 μL of double distilled water and 20 μL of 0.2 mmol/L standard liquid), experimental well (20 μL of culture solution sample), and control well (2 μL of double distilled water and 20 μL of medium). Each well was added with 25 μL of 2, 4-dinitrophenylhydrazine and incubated for 15 min, followed by being added with 250 μL of 0.4 mol/L NaOH solution and incubated for 15 min. OD at 440 nm was measured by a

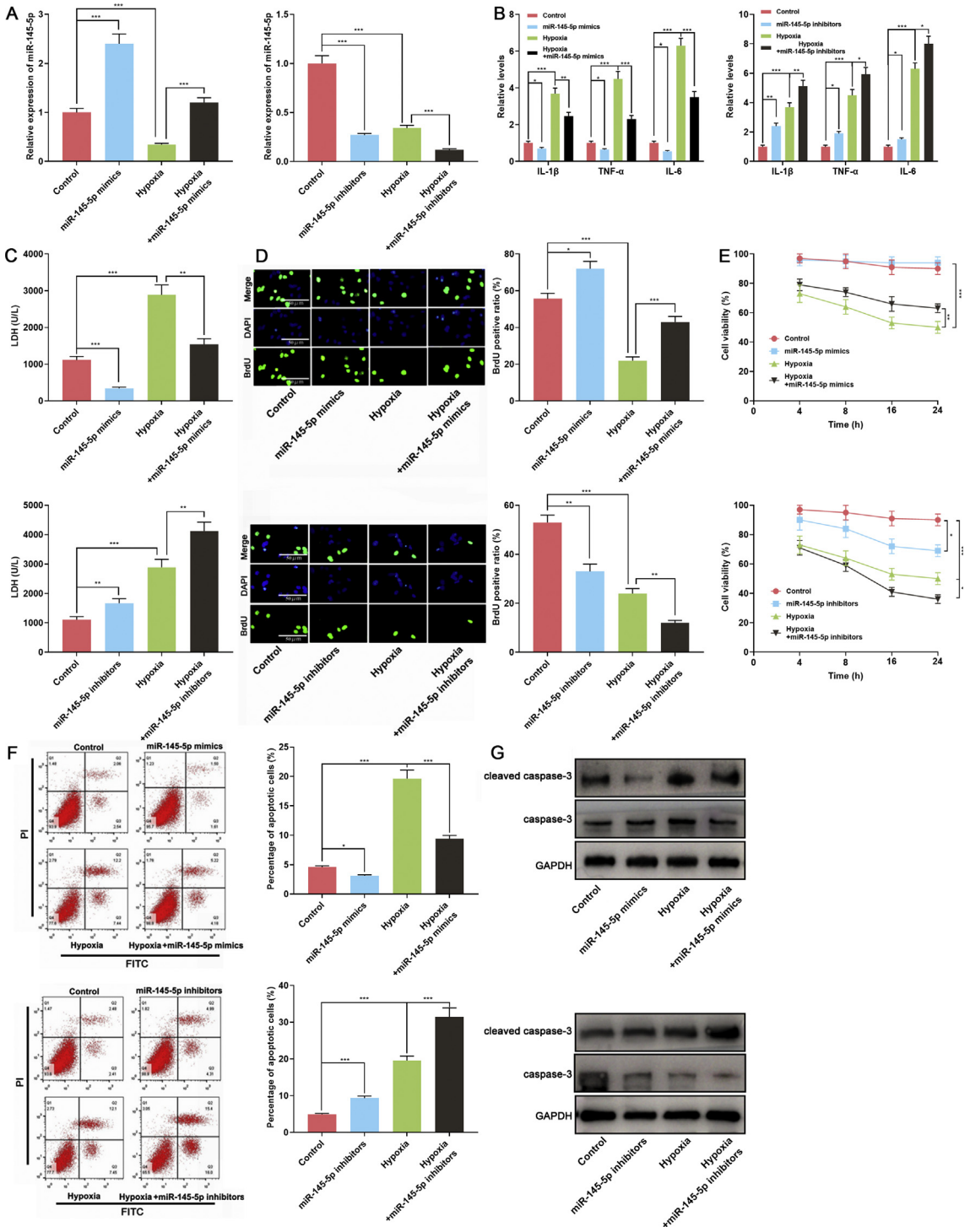

Fig. 2 **The role of miR-145-5p in H9c2 cells.** (A) After the transfection of negative control, miR-145-5p mimics or miR-145-5p inhibitors, H9c2 cells were cultured in normoxia or hypoxia and the transfection efficiency was confirmed by qRT-PCR. (B) The expression levels of IL-1β, TNF-α, and IL-6 in H9c2 cells cultured in normoxia or hypoxia and transfected with miR-145-5p mimics or inhibitors were detected by ELISA. (C) After the transfection of miR-145-5p mimics or inhibitors, LDH release of H9c2 cells in normoxia and hypoxia was detected by the LDH cytotoxicity assay kit. (D) After the transfection of miR-145-5p mimics or inhibitors, the proliferation of H9c2 cells in normoxia and hypoxia was measured with BrdU assay. (E) The viability of H9c2 cells cultured in normoxia or hypoxia following the transfection with miR-145-5p mimics or inhibitors was detected by CCK-8 assay after 4 h, 8 h, 16 h, and 24 h of culture, respectively. (F) Flow cytometry was performed to analyze apoptosis of H9C2 cells cultured in normoxia or hypoxia after the transfection with miR-145-5p mimics or inhibitors. (G) Western blot was used to detect the expression of caspase-3 and cleaved caspase-3. *$p < 0.05$, **$p < 0.01$, and ***$p < 0.001$.

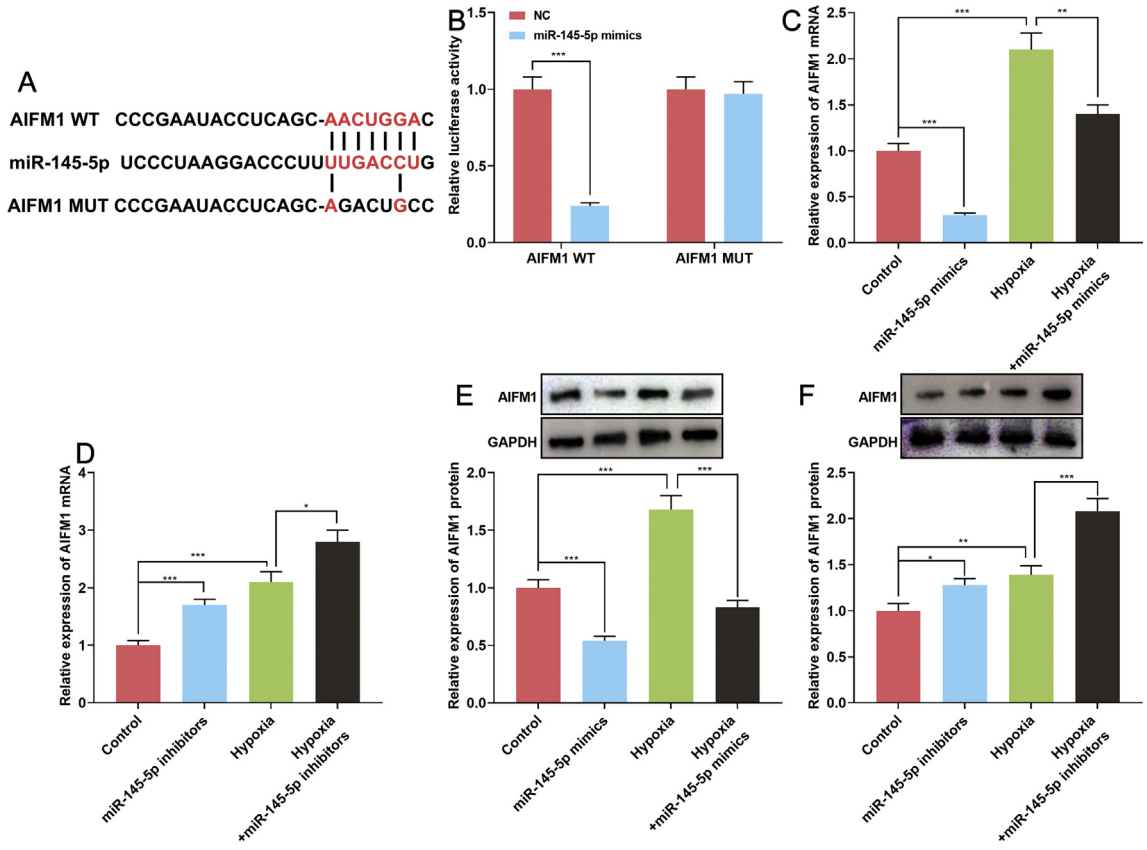

Fig. 3 **The binding relationship between miR-145-5p and AIFM1**. (A) The binding sequence between AIFM1 and miR-145-5p was predicted by TargetScan database. The wild type sequence and mutant type sequence were cloned into pGL3 vector. (B) The binding site between miR-145-5p and AIFM1 was verified by a dual-luciferase reporter assay. (C–F) The expressions of AIFM1 mRNA and protein following the transfection with miR-145-5p mimics or inhibitors were detected by qRT-PCR and Western blot. *$p < 0.05$, **$p < 0.01$, and ***$p < 0.001$.

microplate reader (Bio-Rad Laboratories, Inc., Hercules, CA, USA). LDH activity was calculated as $(OD_{experimental}-OD_{control})/(OD_{standard}-OD_{blank}) \times$ standard sample concentration $\times$ 1000.

Enzyme-linked immunosorbent assay (ELISA)

The expression levels of cytokines TNF-α, IL-1β, and IL-6 were determined by ELISA kit [Multisciences (Lianke) Biotech, Co., Ltd, Hangzhou, China] following the manufacturer's instructions.

Flow cytometry

Apoptosis of H9c2 cells was detected with Annexin V/propidium iodide (PI) double staining method. 5×10^5 cells in each group were collected and washed twice with pre-cooled PBS. The cells were then stained using the Annexin V-FITC/PI Apoptosis Detection Kit (Yeasen Biotech Co., Ltd., Shanghai, China) in the dark according to the manufacturer's instructions. Then the cells were detected by a BD flow cytometer (BD Bioscience, Franklin Lakes, USA). Ultimately, the data were analyzed by Flowjo V10 software (BD Biosciences, Franklin Lake, NJ, USA).

TUNEL staining

After mice were sacrificed, the hearts were harvested and fixed in formalin for 24 h, subsequently embedded in paraffin and sliced (section thickness: 5 μm). TUNEL staining was performed using the TUNEL FITC apoptosis detection kit (Roche, Shanghai, China) following the manufacturer's instructions. The apoptotic cells were labeled with green fluorescence and nuclei were marked with blue fluorescence under confocal microscopy (TCS SP5 AOBS confocal microscopy system, Leica, Germany).

Statistical method

In this study, three technological repetitions were performed for each sample, and three biological repetitions were used for each experiment. The data obtained in this study were statistically analyzed using SPSS 19.0 (SPSS, Inc., Chicago, IL, USA). All the results were expressed as "mean ± standard

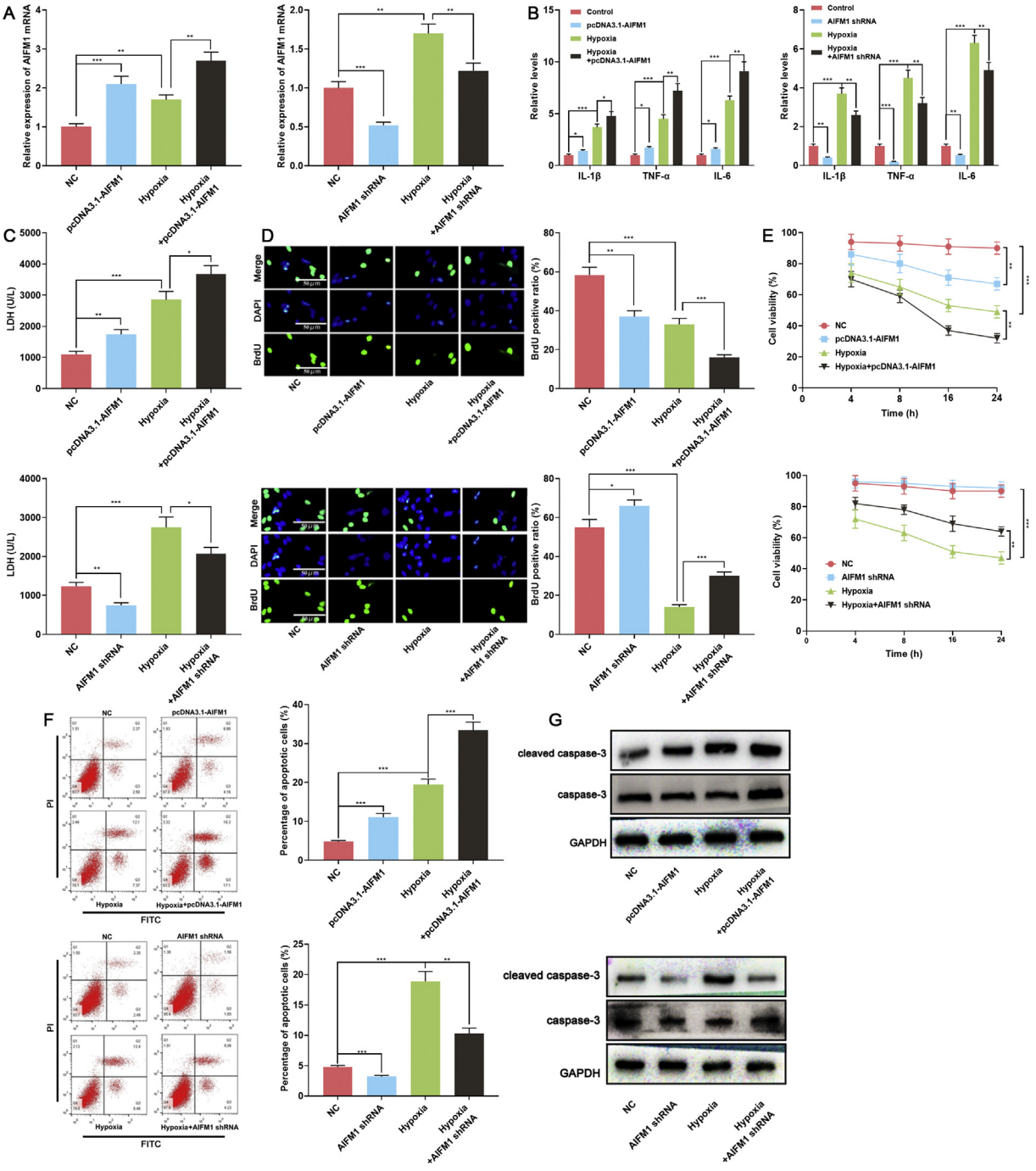

Fig. 4 **The role of AIFM1 in H9c2 cells.** (A) After the transfection of empty vector, control shRNA, pcDNA3.1-AIFM1, or AIFM1 shRNA, H9c2 cells were cultured in normoxia or hypoxia and the transfection efficiency was confirmed by qRT-PCR. (B) The expression levels of IL-1β, TNF-α, and IL-6 in H9c2 cells cultured in normoxia or hypoxia and transfected with pcDNA3.1-AIFM1 or AIFM1 shRNA were detected by ELISA. (C) After the transfection with pcDNA3.1-AIFM1 or AIFM1 shRNA, LDH release of H9c2 cells in normoxia and hypoxia was detected with LDH cytotoxicity assay kit. (D) After the transfection with pcDNA3.1-AIFM1 or AIFM1 shRNA, the proliferation of H9c2 cells in normoxia and hypoxia was measured by BrdU assay. (E) The viability of H9c2 cells cultured in normoxia or hypoxia following the transfection with pcDNA3.1-AIFM1 or AIFM1 shRNA was detected by CCK-8 assay after 4 h, 8 h, 16 h, and 24 h of culture, respectively. (F) Flow cytometry was performed to analyze apoptosis of H9c2 cells cultured in normoxia or hypoxia after the transfection of pcDNA3.1-AIFM1 or AIFM1 shRNA. (G) Western blot was used to detect the expression of caspase-3 and cleaved caspase-3. $*p < 0.05$, $**p < 0.01$, and $***p < 0.001$.

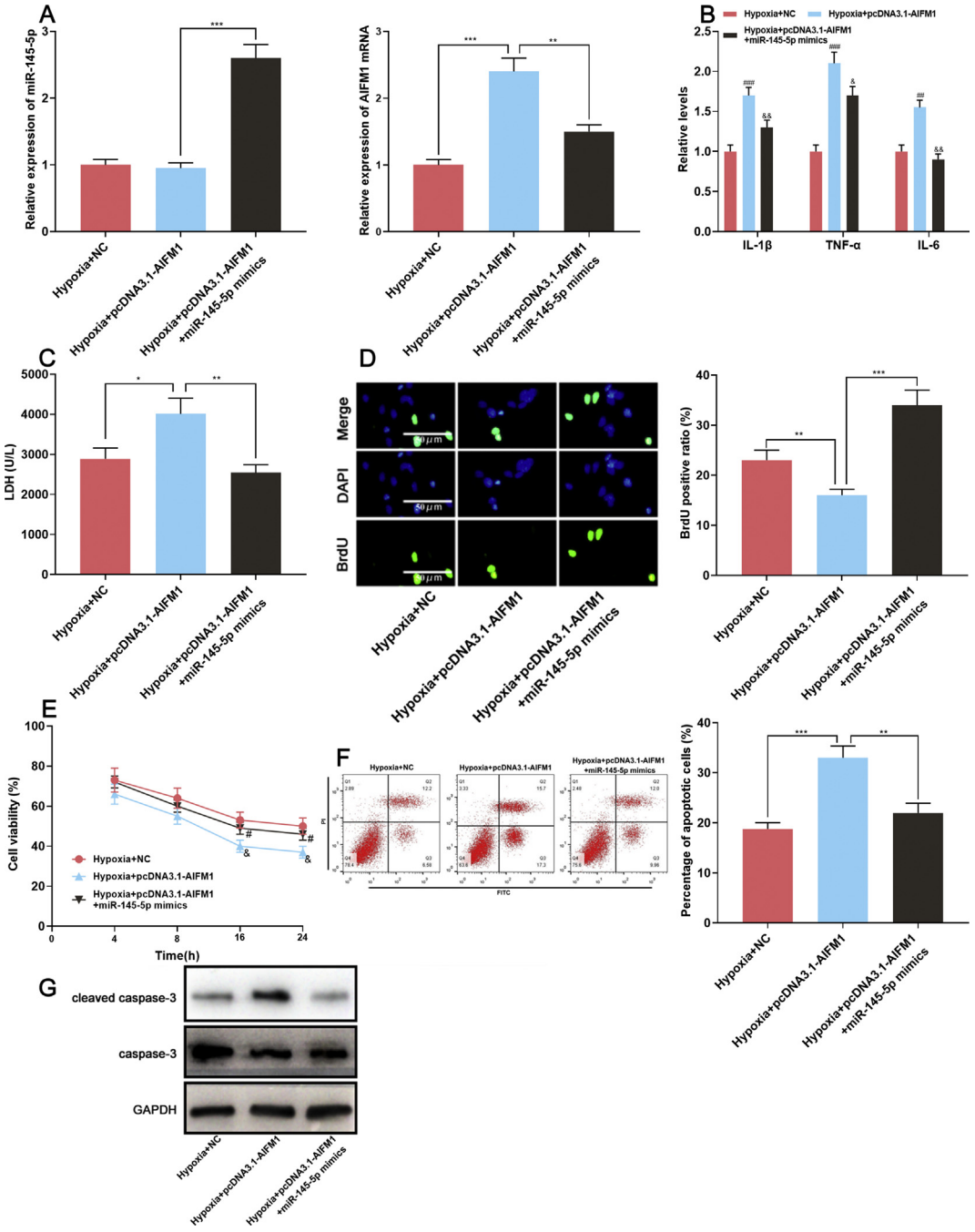

Fig. 5 **miR-145-5p reversed the effect of AIFM1 on H9c2 cells.** (A) After the transfection with pcDNA3.1-AIFM1 or co-transfection with pcDNA3.1-AIFM1 and miR-145-5p mimics, qRT-PCR was employed to verify the expression levels of miR-145-5p and AIFM1 mRNA in hypoxia condition. (B) ELISA indicated that miR-145-5p reversed the role of AIMF1 in promoting the release of inflammatory cytokines from H9c2 cells. (C) LDH release test suggested that miR-145-5p reversed the role of AIFM1 in promoting cell injury. (D) BrdU assay suggested that miR-145-5p reversed the role of AIMF1 in inhibiting the proliferation of H9c2 cells. (E) CCK-8 assay showed that miR-145-5p reversed the role of AIFM1 in reducing the viability of H9c2 cells. (F) Flow cytometry assay demonstrated that miR-145-5p alleviated the role of AIFM1 in promoting the apoptosis of H9c2 cells. (G) Western blot was used to detect the expression of caspase-3 and cleaved caspase-3. *$p < 0.05$, **$p < 0.01$, and ***$p < 0.001$.

deviation" ($\bar{x} \pm s$). For non-normally distributed data, the non-parametrical Wilcoxon sum rank test was used to compare the difference between the two groups. Comparison among multiple groups was performed with Kruskal–Wallis test, and inter-group differences were tested with the Dunn test. Rates and proportions were compared by the Chi-square test. The survival analysis of mice was performed with the Kaplan–Meier method, and the Kaplan–Meier curves were compared with the log-rank test. $p < 0.05$ was considered to be statistically significant.

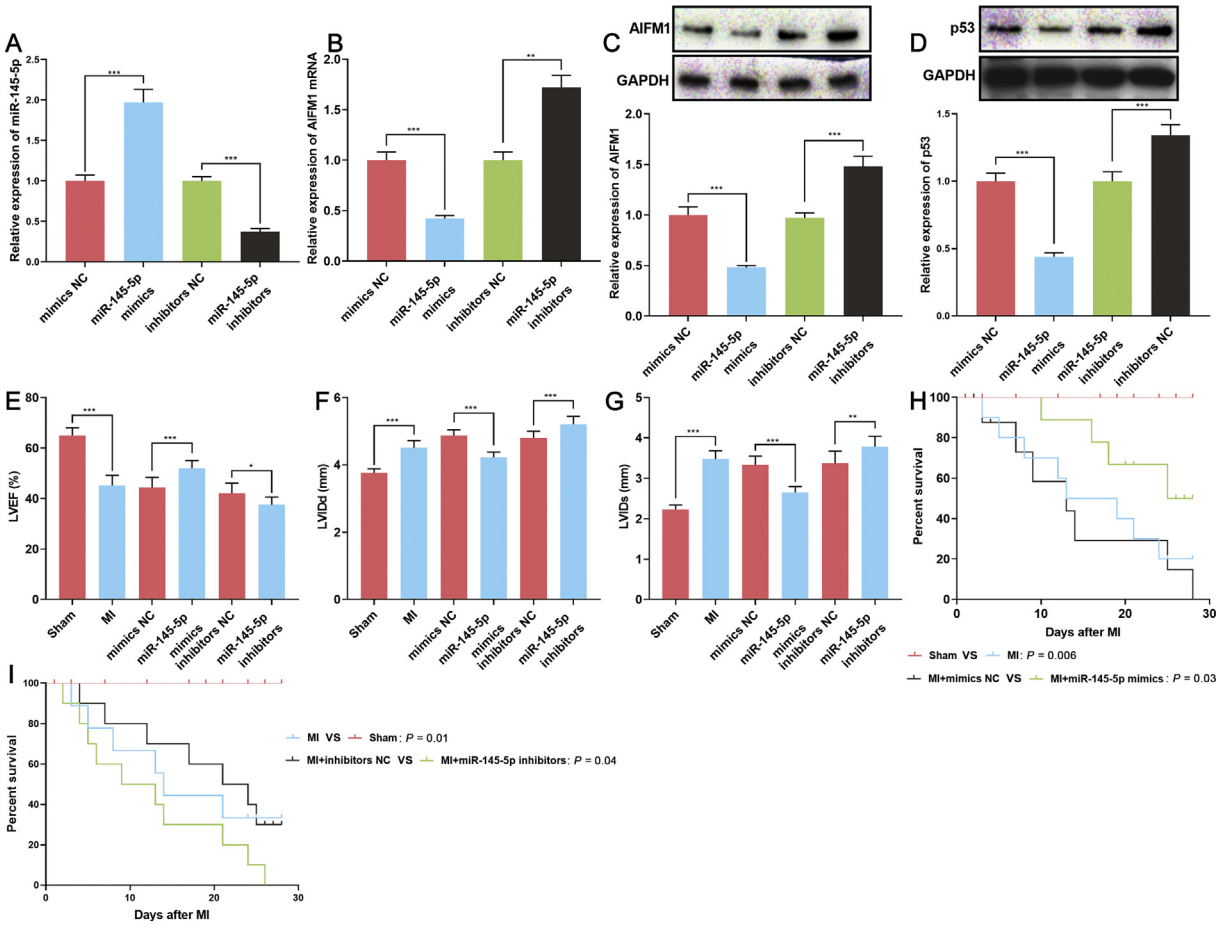

Fig. 6 **The influence of miR-145-5p on mice with MI**. (A–C) Forty mice were injected with mimics control, miR-145-5p mimics, miR-145-5p inhibitors or inhibitors control before left anterior descending coronary artery ligation. qRT-PCR and Western blot were performed to measure the miR-145-5p, AIFM1 mRNA, and protein expressions of myocardial tissue in mice after the mice were sacrificed. (D) The expression level of p53 in mouse myocardial tissue was detected by Western blot. (E–G) The ejection fraction, left ventricular end diastolic diameter (LVIDd), and left ventricular end systolic diameter (LVIDs) of mice were detected after being injected with miR-145-5p mimics or inhibitor and ligation. (H–I) After the injection and ligation, the survival of mice was recorded. $*p < 0.05$, $**p < 0.01$, and $***p < 0.001$. Sham: Sham operation; MI: myocardial infarction.

Results

MiR-145-5p and AIFM1 were abnormally expressed in the mice model of MI and hypoxic H9c2 cells

First of all, we detected the expression levels of miR-145-5p and AIFM1 mRNA in the heart tissues of MI mice and hypoxic H9c2 cells. The result indicated that miR-145-5p expression was markedly decreased in the heart tissues of MI mice, while AIFM1 mRNA expression was significantly increased [Fig. 1A–B]. Consistently, the expression of miR-145-5p was down-regulated in H9c2 cells dependent on hypoxia culture time; AIFM1 mRNA and protein expression in H9c2 cells showed the opposite trend [Fig. 1C–D].

MiR-145-5p alleviated the apoptosis of cardiomyocytes

In order to verify the role of miR-145-5p, we successfully established the models of H9c2 cells with miR-145-5p overexpression or inhibition using miR-145-5p mimics and inhibitors, respectively [Fig. 2A]. The expression levels of hypoxia-related inflammatory cytokines IL-1β, TNF-α, and IL-6 in H9c2 cells were further detected by ELISA, the results of which indicated that hypoxia contributed to the increased expression of these cytokines, while transfection with miR-145-5p mimics reversed the effect of hypoxia and miR-145-5p inhibitor exerted the opposite effects [Fig. 2B]. LDH release assay suggested that miR-145-5p mimics alleviated hypoxia-induced cardiomyocyte injury, while miR-145-5p inhibitor aggravated it [Fig. 2C]. Moreover, BrdU assay suggested that miR-145-5p mimics enhanced the viability of H9c2 cells, while miR-145-5p inhibitors resulted in the opposite result [Fig. 2D]. CCK-8 assay revealed that miR-145-5p mimics increased cell viability, while miR-145-5p inhibitors decreased it [Fig. 2E]. Moreover, transfection of miR-145-5p mimics significantly reduced the apoptosis of H9c2 cells and miR-145-5p inhibitors worked oppositely in both normoxia and hypoxia conditions [Fig. 2F]. Western blot showed that overexpression of miR-145-5p reduced cleaved

caspase-3 expression while inhibiting miR-145-5p exerted the opposite effects [Fig. 2G].

MiR-145-5p targeted AIFM1

To clarify the mechanism of action of miR-145-5p, we searched TargetScan database and discovered that AIFM1, which was closely associated with DNA damage and apoptosis of cells, was one of the potential targets of miR-145-5p [Fig. 3A]. Next, we further confirmed the relationship between AIFM1 3′UTR and miR-145-5p by dual-luciferase reporter assay [Fig. 3B]. To further validate the interaction between AIFM1 and miR-145-5p, we carried out qRT-PCR and Western blot. The results suggested that miR-145-5p mimics could inhibit the expressions of AIFM1 mRNA and protein, whereas miR-145-5p inhibitors increased these expressions in H9c2 cardiomyocytes [Fig. 3C–F].

AIFM1 aggravated the apoptosis of cardiomyocytes

To fathom the role of AIFM1 in cardiomyocytes, pcDNA3.1-AIFM1 and AIFM1 shRNA were transfected into H9c2 cells to increase or decrease AIFM1 expression, respectively [Fig. 4A]. ELISA indicated that AIFM1 overexpression increased the release of inflammatory cytokines, while AIFM1 knockdown decreased this process [Fig. 4B]. LDH release test further confirmed the role of AIFM1 in promoting the injury of H9c2 cells induced by hypoxia [Fig. 4C]. BrdU assay revealed that AIFM1 overexpression reduced the proliferation ability of cells, while the opposite effect could be observed after AIFM1 knockdown [Fig. 4D]. CCK-8 assay showed that AIFM1 overexpression reduced the viability of H9c2 cells, while AIFM1 knockdown increased it [Fig. 4E]. In the meantime, it was demonstrated that AIFM1 overexpression markedly increased the apoptosis of H9c2 cells but AIFM1 shRNA transfection exerted the opposite effects [Fig. 4F]. Moreover, overexpression of AIFM1 promoted cleaved caspase-3 expression, while down-regulated AIFM1 exerted the opposite effect [Fig. 4G]. These results suggested that AIFM1 was an injurious factor during MI.

The biological function of AIFM1 was inhibited by miR-145-5p overexpression

To figure out the functional interaction between AIFM1 and miR-145-5p, H9c2 cells subjected to hypoxia were successfully transfected with pcDNA3.1-AIFM1 or co-transfected with miR-145-5p mimics and pcDNA3.1-AIFM1. The result showed that the transfection with pcDNA3.1-AIFM1 did not affect miR-145-5p expression, suggesting that miR-145-5p exerted a unidirectional regulatory effect on AIFM1 [Fig. 5A]. The result of ELISA showed that the introduction of miR-145-5p mimics reversed the role of AIFM1 overexpression in promoting the release of cytokines IL-1β, TNF-α, and IL-6 [Fig. 5B]. LDH

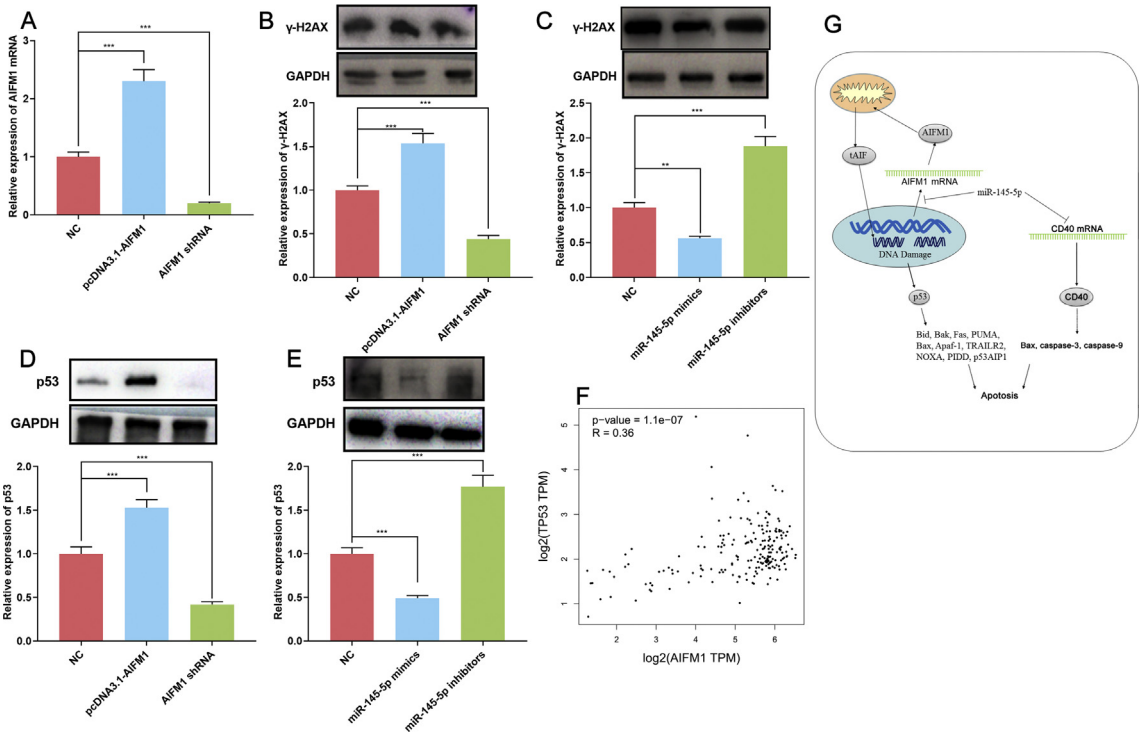

Fig. 7 **The relationship between miR-145-5p/AIFM1 axis and p53**. (A) In normoxia, the expression of AIFM1 mRNA in H9c2 cells transfected with pcDNA3.1-AIFM1 or AIFM1 shRNA was detected by qRT-PCR. (B–E) The expressions of γ-H2AX and p53 after the transfection with pcDNA3.1-AIFM1, AIFM1 shRNA, miR-145-5p mimics, or miR-145-5p inhibitors were tested by Western blot in normoxic condition. (F) It was found in GEPIA database that AIFM1 expression and p53 expression in human left ventricle tissues were positively correlated. (G) Graphic abstract: miR-145-5p/AIFM1/p53 axis and miR-145-5p/CD40 axis in apoptosis of cardiomyocytes. $^{**}p < 0.01$, and $^{***}p < 0.001$.

release test further validated that miR-145-5p reversed the role of AIFM1 in aggravating cell injury [Fig. 5C]. BrdU assay indicated that miR-145-5p mimics reversed the effect of AIFM1 on the viability of H9c2 cells [Fig. 5D]. CCK-8 assay suggested that miR-145-5p also reversed the role of AIFM1 in weakening the viability of H9c2 cells [Fig. 5E]. Through flow cytometry and Western blot, we found that the promoting effects of AIFM1 on apoptosis and the expression of cleaved caspase-3 were alleviated by miR-145-5p mimics co-transfection [Fig. 5F].

The role of miR-145-5p in mice with MI

To further explore the function of miR-145-5p in MI, we injected miR-145-5p mimics or inhibitors into mice via tail vein and then obtained their myocardium to determine the expression levels of AIFM1 mRNA and protein. We confirmed the expression of miR-145-5p in the myocardium was interfered. It was found that AIFM1 expression was decreased after the injection of miR-145-5p mimics and increased after the injection of miR-145-5p inhibitors [Fig. 6A–C], and the change of p53 expression was consistent with that of AIFM1 expression [Fig. 6D]. The cardiac function and left ventricular remodeling of mice were also detected. It was found that, after the mice were injected with miR-145-5p mimics, the ejection fraction of mice was increased, and the left ventricular end-systolic dimension and end-diastolic dimension were reduced while injecting miR-145-5p inhibitors led to the opposite effects [Fig. 6E–G]. Furthermore, we recorded the deaths of mice. It was found that miR-145-5p mimics increased the survival rate of mice (MI + mimics NC vs. MI + miR-145-5p mimics: $p = 0.03$), while miR-145-5p inhibitors decreased it (MI + inhibitors NC vs. MI + miR-145-5p inhibitors: $p = 0.04$) [Fig. 6H–I]. TUNEL staining indicated that the injection with miR-145-5p mimics inhibited apoptosis, while the injection of miR-145-5p inhibitors promoted apoptosis (Supplementary Fig. 1). Thus, with these *in vivo* data, we proved that miR-145-5p had a protective effect on cardiomyocytes by targeting AIFM1 and possibly regulating p53 pathway in the presence of MI.

AIFM1 exerted its biological function via p53 signaling pathway

It is reportedly that AIFM1 causes cell apoptosis by inducing DNA double-strand breaks. To clarify whether AIFM1 participated in regulating myocardial injury in the same way, we transfected H9c2 cells with pcDNA3.1-AIFM1 and AIFM1 shRNA, respectively [Fig. 7A]. Western blot suggested that the transfection with pcDNA3.1-AIFM1 increased the expression level of DNA double-strand breaks marker γ-H2AX, while its knockdown resulted in the opposite result [Fig. 7B]. Moreover, transfection with miR-145-5p mimics and inhibitor led to the down-regulation and up-regulation of γ-H2AX, respectively [Fig. 7C]. In order to further investigate the mechanism of action of AIFM1, we also detected the expression of p53, which was closely associated with DNA damage and repair, and found that AIFM1 positively regulated p53 expression [Fig. 7D], while miR-145-5p negatively modulated it [Fig. 7E]. Moreover, Gene Expression Profiling Interactive Analysis (GEPIA, http://gepia.cancer-pku.cn/) showed the significant correlation between AIFM1 expression and p53 expression in human left ventricle tissues, which was in coincidence with our study [Fig. 7F]. Finally, we confirmed that AIFM1 was specifically regulated by miR-145-5p, and it regulated the injury of cardiomyocytes via modulating p53 signaling pathway [Fig. 7G].

Discussion

MI will result in myocardial remodeling [17], myocardial fibrosis [18], and other adverse effects, and that multiple miRNAs are abnormally expressed in this process and have a protective or destructive effect on cardiomyocytes [19–22]. Considering the fact that mature cardiomyocytes are not reproducible, reducing myocardial injury is one of the potential breakthroughs for the treatment of cardiovascular diseases. Therefore, exploration of specific miRNAs involved in MI has great significance for the identification of new therapeutic targets. In the present study, we found that miR-145-5p expression was abnormally decreased in mice with myocardial ischemia and H9c2 cells subjected to hypoxia. Furthermore, our gain-of-function and loss-of-function experiments confirmed that miR-145-5p could alleviate hypoxia-induced myocardial injury.

Mechanistically, when MI occurs, the apoptotic/necrotic cells will release proteins that can cause myocardial injury and result in systemic inflammatory response. When eliminating the apoptotic/necrotic cells, inflammatory cells will promote the occurrence of myocardial fibrosis, aggravate cell apoptosis, and even cause arrhythmia [23]. When cardiomyocytes were exposed under ischemia-hypoxia, increased glycolysis in cells will cause the accumulation of lactic acid and finally lead to acidosis of the cells, which will further exacerbate the apoptosis of cardiomyocytes [24]. The findings of our study showed that miR-145-5p inhibited the generation of inflammatory cytokines following hypoxic myocardial injury, further suggesting that miR-145-5p might play a pivotal role in myocardial injury.

In recent years, accumulating studies show that miRNA exerts a crucial role in the process of hypoxic-ischemic myocardial injury and has an important influence on the apoptosis, viability, inflammatory response, and other biological processes of cardiomyocytes. For example, miR-130a targets Smad4 and inhibits hypoxia-induced myocardial apoptosis [25]; In C57BL/6 mice with MI, the up-regulation of miR-7a/b inhibits cardiomyocytes' apoptosis [26]; miR-9 represses the proliferation of cardiomyocytes via repressing YAP1 [27]; miR-21 is found to repress the release of inflammatory cytokines in the cardiomyocytes of mice with MI [28]. In the present study, we found that miR-145-5p was abnormally expressed in the presence of MI. Furthermore, we established a mouse model of MI and a hypoxia model of H9c2 cells by coronary artery ligation and hypoxic culture, respectively. The abnormal low expression of miR-145-5p was observed in a hypoxic condition, and transfection with miR-145-5p mimics could improve the viability of H9c2 cells.

After the mice with MI were injected with miR-145-5p mimics, the myocardial remodeling was ameliorated, and cardiac function was significantly improved. Besides, some studies report that miR-145-5p plays a role in hypertension and other cardiovascular diseases. For instance, miR-145-5p can negatively regulate Bnip3 to reduce the damage to H9c2 cells in a hypoxic condition [29]. MiR-145-5p directly targeted CD40, inhibiting the expression of Bax, caspase-3, and caspase-9, alleviating hypoxia-induced inflammatory response and apoptosis in cardiomyocytes [30]. MiR-145-5p activated mTOR and MEK/ERK pathways, thereby protected cardiomyocytes from oxygen-glucose-deprivation -induced injury [31]. These studies suggest that miR-145-5p is a protective factor for cardiomyocytes, which is consistent with the result of our study.

In this study, we demonstrated that AIFM1was one of the downstream targets of miR-145-5p, and could be negatively regulated by it. Physiologically, AIFM1 is located in mitochondria and regulates electron transport, ferredoxin metabolism, reactive oxygen species generation, and ATP production [15]. AIFM1 can promote apoptosis via promoting pro-apoptotic genes such as caspase3 and DRAM [32]. The dysregulation of AIFM1 is reported to be associated with some human diseases. For example, AIFM1 can promote the apoptosis of tumor cells and be specifically regulated by miR-425-5p in cervical cancer [33]. In our study, AIFM1 was found to be abnormally expressed in the myocardial tissue of mice with MI and H9c2 cells subjected to hypoxia. We also unveiled that AIFM1 overexpression reduced the viability of H9c2 cells and aggravated their inflammatory response and cell injury, while AIFM1 knockdown showed the opposite effects. The result of Western blot indicated that AIFM1 triggered cell apoptosis by affecting DNA double-strand breaks. Our further investigation suggested that p53 expression was positively regulated by AIFM1. These data indicated that AIFM1, an important factor in the presence of myocardial injury, played a role in aggravating hypoxia-induced myocardial injury and probably exerted its biological function via p53 signaling pathway.

Conclusion

Collectively, we report that miR-145-5p targets AIFM1 and regulates the apoptosis of cardiomyocytes via p53 signaling pathway. We also find that miR-145-5p and AIFM1 are involved in regulating cardiac function and cardiac remodeling after MI. This work helps explain the molecular mechanism of myocardial injury and provides potential therapeutic targets for MI.

Ethics approval and consent to participate

Animal experiments were approved by the Animal Care and Use Committee of Shanghai Ninth People's Hospital.

Consent for publication

Not applicable.

Availability of data and material

The data used to support the findings of this study are available from the corresponding author upon request.

Funding

The study was supported by 2020 Natural Science Foundation of Tibet Autonomous Region [group-style aid to Tibet, project number: XZ2020ZR-ZY40(Z)].

Conflicts of interest

The authors declare that they have no competing interests.

Acknowledgement

Not applicable.

Appendix A. Supplementary data

Supplementary data to this article can be found online at https://doi.org/10.1016/j.bj.2021.11.012.

REFERENCES

[1] Reed GW, Rossi JE, Cannon CP. Acute myocardial infarction. Lancet 2017;389:197–210.
[2] Cai J, Yu S, Pei Y, Peng C, Liao Y, Liu N, et al. Association between airborne fine particulate matter and residents' cardiovascular diseases, ischemic heart disease and cerebral vascular disease mortality in areas with lighter air pollution in China. Int J Environ Res Publ Health 2018;15:1918.
[3] Xie W, Li G, Zhao D, Xie X, Wei Z, Wang W, et al. Relationship between fine particulate air pollution and ischaemic heart disease morbidity and mortality. Heart 2015;101:257–63.
[4] Cahill TJ, Choudhury RP, Riley PR. Heart regeneration and repair after myocardial infarction: translational opportunities for novel therapeutics. Nat Rev Drug Discov 2017;16:699–717.
[5] Bejarano J, Navarro-Marquez M, Morales-Zavala F, Morales JO, Garcia-Carvajal I, Araya-Fuentes E, et al. Nanoparticles for diagnosis and therapy of atherosclerosis and myocardial infarction: evolution toward prospective theranostic approaches 2018;8:4710–32.
[6] Wang K, Liu CY, Zhou LY, Wang JX, Wang M, Zhao B, et al. APF lncRNA regulates autophagy and myocardial infarction by targeting miR-188-3p. Nat Commun 2015;6:6779.
[7] Yang Y, Cheng HW, Qiu Y, Dupee D, Noonan M, Lin YD, et al. MicroRNA-34a plays a key role in cardiac repair and regeneration following myocardial infarction. Circ Res 2015;117:450–9.
[8] Wang K, Liu F, Liu CY, An T, Zhang J, Zhou LY, et al. The long noncoding RNA NRF regulates programmed necrosis and myocardial injury during ischemia and reperfusion by targeting miR-873. Cell Death Differ 2016;23:1394–405.

[9] Shi L, Tian C, Sun L, Cao F, Meng Z. The lncRNA TUG1/miR-145-5p/FGF10 regulates proliferation and migration in VSMCs of hypertension. Biochem Biophys Res Commun 2018;501:688–95.
[10] Li L, Mao D, Li C, Li M. miR-145-5p inhibits vascular smooth muscle cells (VSMCs) proliferation and migration by dysregulating the transforming growth factor-b signaling cascade. Med Sci Monit 2018;24:4894–904.
[11] Yuan M, Zhang L, You F, Zhou J, Ma Y, Yang F, et al. MiR-145-5p regulates hypoxia-induced inflammatory response and apoptosis in cardiomyocytes by targeting CD40. Mol Cell Biochem 2017;431:123–31.
[12] Wu G, Tan J, Li J, Sun X, Du L, Tao S. miRNA-145-5p induces apoptosis after ischemia-reperfusion by targeting dual specificity phosphatase 6. J Cell Physiol 2019;234:16281–9.
[13] Bano D, Prehn JHM. Apoptosis-inducing factor (AIF) in physiology and disease: the tale of a repented natural born killer. EBioMedicine 2018;30:29–37.
[14] Kettwig M, Schubach M, Zimmermann FA, Klinge L, Mayr JA, Biskup S, et al. From ventriculomegaly to severe muscular atrophy: expansion of the clinical spectrum related to mutations in AIFM1. Mitochondrion 2015;21:12–8.
[15] Morton SU, Prabhu SP, Lidov HGW, Shi J, Anselm I, Brownstein CA, et al. AIFM1 mutation presenting with fatal encephalomyopathy and mitochondrial disease in an infant. Cold Spring Harb Mol Case Stud 2017;3:a001560.
[16] Zhao G, Wang S, Wang Z, Sun A, Yang X, Qiu Z, et al. CXCR6 deficiency ameliorated myocardial ischemia/reperfusion injury by inhibiting infiltration of monocytes and IFN-gamma-dependent autophagy. Int J Cardiol 2013;168:853–62.
[17] Wei DZ, Lin C, Huang YQ, Wu LP, Huang MY. Ellagic acid promotes ventricular remodeling after acute myocardial infarction by up-regulating miR-140-3p. Biomed Pharmacother 2017;95:983–9.
[18] Yuan J, Chen H, Ge D, Xu Y, Xu H, Yang Y, et al. Mir-21 promotes cardiac fibrosis after myocardial infarction via targeting Smad7. Cell Physiol Biochem 2017;42:2207–19.
[19] Liu Y, Wang H, Wang X, Xie G. MiR-29b inhibits ventricular remodeling by activating notch signaling pathway in the rat myocardial infarction model. Heart Surg Forum 2019;22:E019–23.
[20] Chen Y, Li T, Gao Q, Wang LY, Cui LQ. MiR-1908 improves cardiac fibrosis after myocardial infarction by targeting TGF-β1. Eur Rev Med Pharmacol Sci 2018;22:2061–9.
[21] Díaz I, Calderón-Sánchez E, Toro RD, Ávila-Médina J, de Rojas-de Pedro ES, Domínguez-Rodríguez A, et al. miR-125a, miR-139 and miR-324 contribute to Urocortin protection against myocardial ischemia-reperfusion injury. Sci Rep 2017;7:8898.
[22] Tian ZQ, Jiang H, Lu ZB. MiR-320 regulates cardiomyocyte apoptosis induced by ischemia-reperfusion injury by targeting AKIP1. Cell Mol Biol Lett 2018;23:41.
[23] Huang S, Frangogiannis NG. Anti-inflammatory therapies in myocardial infarction: failures, hopes and challenges. Br J Pharmacol 2018;175:1377–400.
[24] Kim DK, Choi E, Song BW, Cha MJ, Ham O, Lee SY, et al. Differentially regulated functional gene clusters identified in early hypoxic cardiomyocytes. Mol Biol Rep 2012;39:9549–56.
[25] Li Y, Du Y, Cao J, Gao Q, Li H, Chen Y, et al. MiR-130a inhibition protects rat cardiac myocytes from hypoxia-triggered apoptosis by targeting Smad4. Kardiol Pol 2018;76:993–1001.
[26] Geng HH, Li R, Su YM, Xiao J, Pan M, Cai XX, et al. Curcumin protects cardiac myocyte against hypoxia-induced apoptosis through upregulating miR-7a/b expression. Biomed Pharmacother 2016;81:258–64.
[27] Zheng J, Peng B, Zhang Y, Ai F, Hu X. miR-9 knockdown inhibits hypoxia-induced cardiomyocyte apoptosis by targeting Yap1. Life Sci 2019;219:129–35.
[28] Yang L, Wang B, Zhou Q, Wang Y, Liu X, Liu Z, et al. MicroRNA-21 prevents excessive inflammation and cardiac dysfunction after myocardial infarction through targeting KBTBD7. Cell Death Dis 2018;9:769.
[29] Wu Z, Zhao S, Li C, Liu C. LncRNA TUG1 serves an important role in hypoxia-induced myocardial cell injury by regulating the miR-145-5p-Binp3 axis. Mol Med Rep 2018;17:2422–30.
[30] Yuan M, Zhang L, You F, Zhou J, Ma Y, Yang F, et al. MiR-145-5p regulates hypoxia-induced inflammatory response and apoptosis in cardiomyocytes by targeting CD40. Mol Cell Biochem 2017;431:123–31.
[31] Jin Q, Chen Y. Silencing circular RNA circ_0010729 protects human cardiomyocytes from oxygen-glucose deprivation-induced injury by up-regulating microRNA-145-5p. Mol Cell Biochem 2019;462:185–94.
[32] Liu D, Liu M, Wang W, Pang L, Wang Z, Yuan C, et al. Overexpression of apoptosis-inducing factor mitochondrion-associated 1 (AIFM1) induces apoptosis by promoting the transcription of caspase3 and DRAM in hepatoma cells. Biochem Biophys Res Commun 2018 Apr 6;498:453–7.
[33] Zhang Y, Yang Y, Liu R, Meng Y, Tian G, Cao Q. Downregulation of microRNA-425-5p suppresses cervical cancer tumorigenesis by targeting AIFM1. Exp Ther Med 2019;17:4032–8.